

# The Important Role Played by High-Temperature Tensile Testing in the Representation of Minimum Creep Rates Using S-Shaped Curve Models



M. EVANS

It is important to characterize the creep life of materials used in power plants and aeroengines. This paper illustrates the important role played by a material's tensile strength in enabling accurate creep property representations to be made. It also shows that published high-temperature tensile strength values are not always suitable for use in certain creep models due to its strain rate dependency. To deal with the absence of such suitable data on tensile strength, this paper estimates such values directly from minimum creep rate data. When this technique is applied to models that represent the relationship between minimum creep rates and normalized (with respect to tensile strength) stress using S-shaped curves, an improvement in the fit to data on 2.25Cr–1Mo steel was observed. The findings suggest an important need for future research into the most appropriate strain rates to be used in high-temperature tensile testing when the purpose is to use the resulting tensile strength values for use in creep modeling.

<https://doi.org/10.1007/s11661-023-07202-w>  
© The Author(s) 2023

## I. INTRODUCTION

ALTHOUGH complex stresses and temperatures are often encountered by materials used in power generation, design decisions are generally made on the basis of an “allowable” tensile creep strength. This strength is commonly taken to be 67 pct of the average stress (up to 1088 K).<sup>[1]</sup> Currently, expensive testing lasting 12 to 15 years is required to determine the long-term strengths and lives. A reduction in this ‘materials development cycle’ was therefore defined as the No. 1 priority in the 2007 UK Energy Materials—Strategic Research.<sup>[2]</sup> With the aim of reducing this development cycle, a new group of parametric creep models have been developed in recent years that are characterized through their use of an S-shaped curve to describe the relationship between the minimum creep rate and a normalized stress at a fixed temperature. In these models,  $\sigma_{\max}$  is defined as stress that will induce—in practical terms—instantaneous creep rupture when it is instantly applied (so inducing a very high strain rate) to a specimen in a creep test. It follows therefore that  $\sigma_{\max}$  can be taken as the tensile strength as measure through a standard high-temperature tensile test, subject to the condition

that such a test is conducted at a sufficiently high strain rate. These S-shaped curve models are further characterized by the fact that they contain some sensible boundary conditions. Namely, when  $\sigma = \sigma_{\max}$  failure will occur instantaneously and as the stress approaches zero, the time to failure tends to become infinitely large. These should be viewed as mathematical conditions characteristic of the creep model equation because given the Monkman–Grant<sup>[3]</sup> relation, a failure time approaching zero implies a minimum creep rate approaching infinity, which has no current physical basis.

Evans<sup>[4]</sup> recently specified a mathematical model that encompasses two of these S-shaped curve models that are present in the literature on creep

$$\dot{\epsilon}_M = A\tau^{-n} \exp\left\{\frac{-Q_c}{RT}\right\} \quad \text{where } \tau = \left[k\left(\frac{\sigma}{\sigma_{\max}}\right)^{-1/k} - k\right], \quad [1a]$$

where  $\dot{\epsilon}_M$  is the minimum creep rate,  $R$  is the universal gas constant,  $\sigma$  stress,  $T$  is absolute temperature, and  $Q_c$  is the activation energy for creep.  $A$  and  $n$  are additional model parameters. This model is characterized by an S-shaped relationship between  $\dot{\epsilon}_M$  and  $\sigma/\sigma_{\max}$  at constant temperature with boundaries  $\dot{\epsilon}_M \rightarrow \infty$  as  $\sigma/\sigma_{\max} \rightarrow 1$  and  $\dot{\epsilon}_m \rightarrow 0$  as  $\sigma/\sigma_{\max} \rightarrow 0$ , provided  $n > 0$ . When  $k = 1$ ,  $\tau^{-n} = \left[\frac{\sigma}{\sigma_{\max} - \sigma}\right]^n$  and so

M. EVANS is with the Institute of Structural Materials, Swansea University, Fabian Way, Crymlyn Burrows, Wales, SA1 8EN, UK. Contact e-mail: m.evans@swansea.ac.uk

Manuscript submitted May 17, 2023; accepted September 7, 2023.

$$\dot{\epsilon}_M = A \left[ \frac{\sigma}{\sigma_{\max} - \sigma} \right]^n \exp \left\{ \frac{-Q_c}{RT} \right\}. \quad [1b]$$

Equation [1b] is the creep model put forward by Yang *et al.*<sup>[5]</sup> and Wang *et al.*<sup>[6]</sup> and at constant temperature describes a logistic S-shaped curve. Hence, this paper will refer to this as the Logistic S curve model. Then as  $k \rightarrow \infty$ ,  $\tau^{-n} \rightarrow \left[ -\ln \left( \frac{\sigma}{\sigma_{\text{TS}}} \right) \right]^{-n}$ , and so

$$\dot{\epsilon}_M = A \left[ -\ln \left( \frac{\sigma}{\sigma_{\text{TS}}} \right) \right]^{-n} \exp \left\{ \frac{-Q_c}{RT} \right\}. \quad [1c]$$

Equation [1c] is the creep model first put forward by Wilshire and Battenbough<sup>[7]</sup> and at constant temperature describes a Weibull S-shaped curve. Consequently, this will be referred to as the Weibull S curve model.  $k$  can also be rescaled to fall within the limits 0 to 1 through the transformation  $k^* = k^{-0.5}$  (so that when  $k = 1$ ,  $k^* = 1$  and as  $k \rightarrow \infty$ ,  $k^* \rightarrow 0$ ). This rescaling helps in the process of estimating a value for  $k$ . The creep model given by Eq. [1a] will be termed an S-shaped curve model as it incorporates a variety of different S-shaped curves (the shape being determined by the value for  $k$ ) to describe the relationship between  $\dot{\epsilon}_M$  and  $\sigma/\sigma_{\max}$  at constant temperature.

Once a prediction for  $\dot{\epsilon}_M$  has been made using Eq. [1a], the Monkman–Grant<sup>[3]</sup> relation can then be used to convert this to a failure time provided this relation is stable over time

$$t_F = M \dot{\epsilon}_M^\rho \text{ where } \rho < 0, \quad [1d]$$

where  $M$  and  $\rho$  are model constants.

In applications of these S-shaped curve models, most researchers have used  $\sigma_{\text{TS}}$  values supplied by the same testing institutes that generated the uniaxial creep curves. For example, NIMS Creep Data Sheet 3B<sup>[8]</sup> published by the Japanese National Institute for Materials Science (NIMS) contains minimum creep rates for 2.25Cr–1Mo obtained from constant load uniaxial tests, and the same sheet has high-temperature tensile test results (and thus  $\sigma_{\text{TS}}$  values) conducted at a constant strain rate of  $0.00125 \text{ s}^{-1}$ . Researchers have tended to use these  $\sigma_{\text{TS}}$  values to define  $\sigma_{\max}$  in S-shaped curve models. However, there is some evidence in the literature to suggest that a strain rate of  $0.00125 \text{ s}^{-1}$  for this material may be too low and not appropriate for use in Eq. [1a]. However, it is often not possible to use such additional and extraneous tensile strength data because i. there are mismatches between temperatures and ii. the chemical composition and heat treatments of the batches used in the extraneous data sets are different from that in the creep data set.

Consequently, the aim of this paper is then to try and estimate an appropriate value for  $\sigma_{\max}$  directly from the creep data itself—so removing the need to use tensile

strengths. This can be done by treating  $\sigma_{\max}$  as just another parameter to be estimated in the S-shaped curve model of Eq. [1a]. That is,  $\sigma_{\max}$  is obtained from actual minimum creep rates, by finding a value that makes the minimum creep rates most consistent with the constraint in the S-shaped curve model that infinite minimum creep rates occur when  $\sigma = \sigma_{\max}$ . The paper is therefore structured as follows. The next contains more information on the NIMS creep data set and some additional extraneous tensile testing data sets. It is followed by a section reviewing the strain rate dependency in high-temperature tensile testing. There then follows two sections outlining a way to estimate  $\sigma_{\max}$  from Eq. [1a] and detailing the results of applying this method to all the NIMS creep data on minimum creep rates. A conclusion section then gives some recommendations for future work.

## II. EXPERIMENTAL DATA

### A. Japanese National Institute for Materials Science (NIMS) Data

This paper makes use of information in NIMS Creep Data Sheets 3B & 50A, published by the Japanese National Institute for Materials Science (NIMS).<sup>[8,11]</sup> These sheets have extensive data on twelve batches of 2.25Cr–1Mo (according to ASTM A 387, Grade 22) steel where each batch has a different chemical composition that underwent one of four different heat treatments—details of which are given in Reference 8. One batch (and only one) of this 2.25Cr–1Mo steel, the MAF batch, has measurements on minimum creep rates. The testing material was in tube form that had an outside diameter of 50.8 mm, a wall thickness of 8 mm, and a length of 5000 mm with a chemical composition and heat treatment as shown in Table I. Specimens for tensile testing were taken longitudinally from this material. Each test specimen had a diameter of 6 mm with a gauge length of 30 mm. The high-temperature tensile tests carried out on these specimens were obtained using a strain rate of 0.005 pct/s up to 1 pct proof stress and then at 0.125 pct/s until failure. The lower of these two strain rates are applied over mainly, but not exclusively, the elastic deformation range and hence can be discounted.

NIMS Creep Data Sheet 3B and 50A<sup>[8,11]</sup> also contains constant load creep test results. This paper only uses creep results from the MAF batch. Figure 1 plots the minimum creep rates obtained for the MAF batch at the different stresses and temperatures used by NIMS. The relationship between the minimum creep rate and the test conditions is quite complicated for this batch, which has made it very difficult to model and predict such rates using parametric creep models. (The data point circled at 923 K has a failure time of 5080 hours associated with it and this is the only point

**Table I. Chemical Composition for Different Batches of 2.25Cr–1Mo Steel (Pct/Wt)**

Source	Cr	Mo	C	Si	Mn	P	S	Ni	Cu	Al
MAF <sup>[8]</sup>	2.46	0.94	0.1	0.23	0.43	0.011	0.009	0.008	0.07	0.005
Bueno and Sobrinho <sup>[9]</sup>	2.09	1.08	0.097	0.32	0.50	0.007	0.002	0.03	0.01	0.05
Klueh and Oakes <sup>[10]</sup>	2.17	0.91	0.12	0.33	0.56	0.001	0.015	0.16	—	—

Balance Fe. The material used in Ref. [8] was normalized and tempered by heating for 20 minutes at 930 °C and then air cooled; it was tempered for 130 minutes at 720 °C and again air cooled. The material used in Ref. [10] was normalized and tempered by heating for 1 hour at 927 °C and then air cooled; it was tempered for 1 hour at 704 °C and again air cooled.

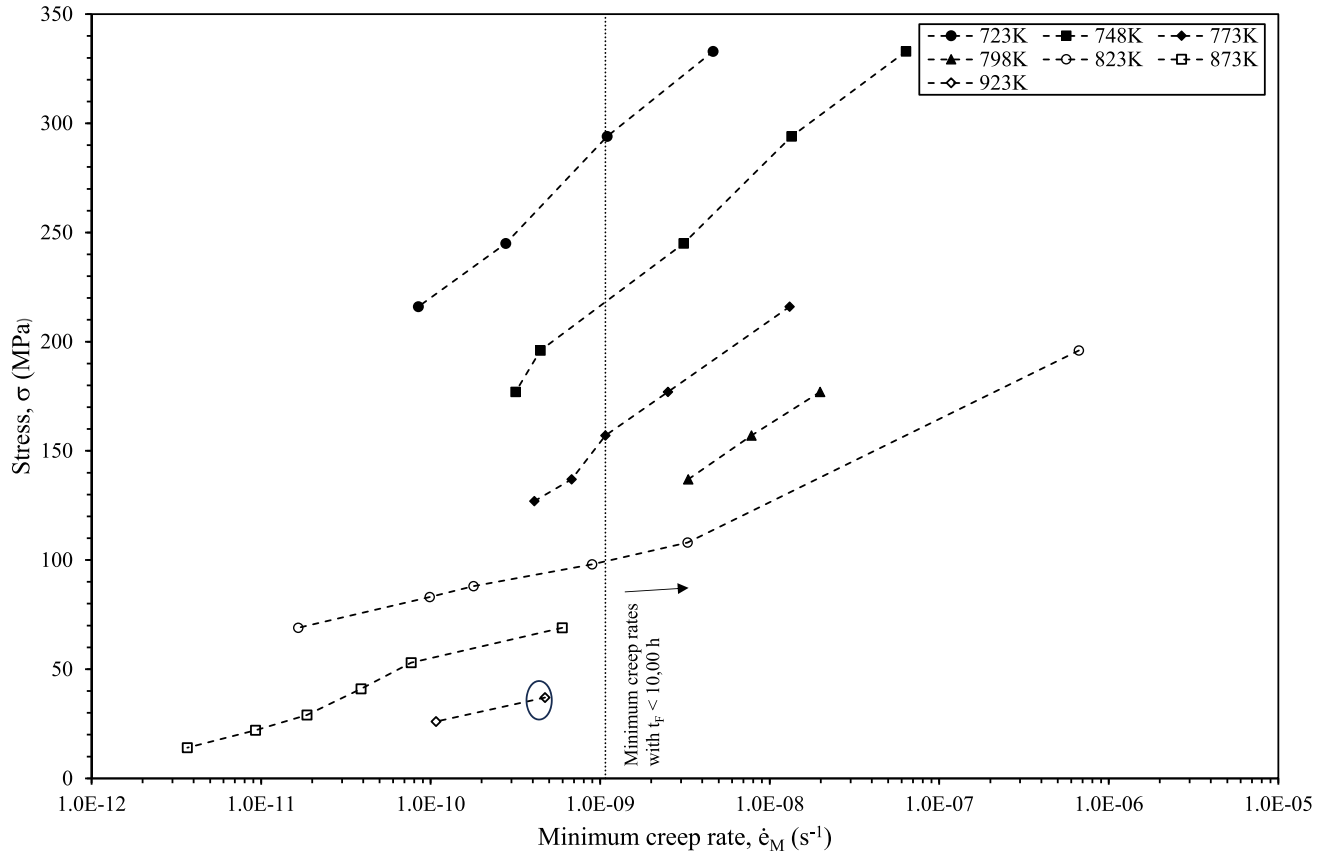


Fig. 1—Relationship between stress, temperature, and minimum creep rates for the MAF batch of 2.25Cr–1Mo steel contained in NIMS creep data sheet 3B and 50A.<sup>[8,11]</sup>

not conforming to the split described by the vertical dotted line.)

### B. Some extraneous data

The first set of extraneous data on high-temperature tensile properties for 2.25Cr–1Mo steel is published by Bueno and Sobrinho.<sup>[9]</sup> The steel used for testing was supplied in plate form with 25.4 mm thickness in the normalized and tempered condition. Table I gives more information on its chemical composition. Metallographic analysis indicated the presence of 30 pct bainite and 70 pct ferrite. This material was tested at strain rates up to 0.01 s<sup>-1</sup>. The tensile specimens were extracted from the rolling direction. A gauge length of 25 mm and an initial diameter of 6.25 mm were used. The second set

of extraneous data on high-temperature tensile properties for 2.25Cr–1Mo steel is published by Klueh and Oakes.<sup>[10]</sup> The steel used for testing was supplied in plate form with 25 mm thickness. Table I gives more information on its chemical composition and heat treatment and the microstructure after this treatment was entirely bainite. This material was tested at strain rates up to 144 s<sup>-1</sup>.

### III. STRAIN RATE DEPENDENCY

Figure 2 shows the tensile strength measurements made by NIMS for the MAF batch of steel. These measurements were obtained using a constant strain rate of 0.00125 s<sup>-1</sup>. From the figure it is observed that there

is a complex temperature dependency, but over the typical creep temperature range the tensile strength drops off with increasing temperature. Figure 3(a) shows the  $\sigma_{TS}$  values obtained by Bueno and Sobrinho<sup>[9]</sup> (digitized from a figure in their paper and so are to be viewed as approximate values). Due in part to the differing chemical compositions and heat treatments, the measured tensile strengths at a comparable strain rate are about 100 MPa higher than in the NIMS data set. For all temperatures (except perhaps for the lowest shown temperature), the tensile strength continues to rise for strain rates that are higher than that used by NIMS. The Klueh and Oakes<sup>[10]</sup> data shown in Figure 3(b) were obtained at even higher strain rates up to  $144 \text{ s}^{-1}$ . Again their measurements are around 100 MPa higher than the NIMS results at a comparable strain rate. Their data reveal that the tensile strength continues to rise above the maximum value used by Bueno and Sobrinho<sup>[9]</sup> and indeed continues to rise as the strain rate increases to  $144 \text{ s}^{-1}$  at higher temperatures.

The two extraneous data sets tend to suggest that the NIMS tensile measurements are inappropriate to use for  $\sigma_{max}$  in Eq. [1a] because they are too low in value—due to using a strain that is too low. Unfortunately, the data

in Figure 3 cannot be used instead because they are much higher in value at the comparable strain rate of  $0.00125 \text{ s}^{-1}$  (due to that data having a different heat treatment and chemical composition). There is also a mismatch in temperatures as well. Hence, the need to try an estimate  $\sigma_{max}$  directly from the creep data itself.

#### IV. METHOD FOR ESTIMATING THE PARAMETERS OF S-SHAPED CURVE MODELS

##### A. The Activation Energy for Creep, $Q_c$

The first step to fully quantify the model given by Eq. [1a] is to determine the activation energy for creep— $Q_c$ . Equation [1a] suggests that  $Q_c$  must be determined from measuring the  $\dot{\epsilon}_M$  values at different temperatures by keeping the stress ratio  $\sigma/\sigma_{max}$  constant. None of the creep rupture data in Reference 8 were deliberately measured under this condition. But, by analyzing the NIMS data set, it was possible to identify five sets of data that approximately meet the condition that  $\sigma/\sigma_{TS}$  is constant. These data sets are shown in Figure 4 which plots  $\ln \dot{\epsilon}_M$  against  $1000/RT$ . The numbers shown at the end points of the best fit lines

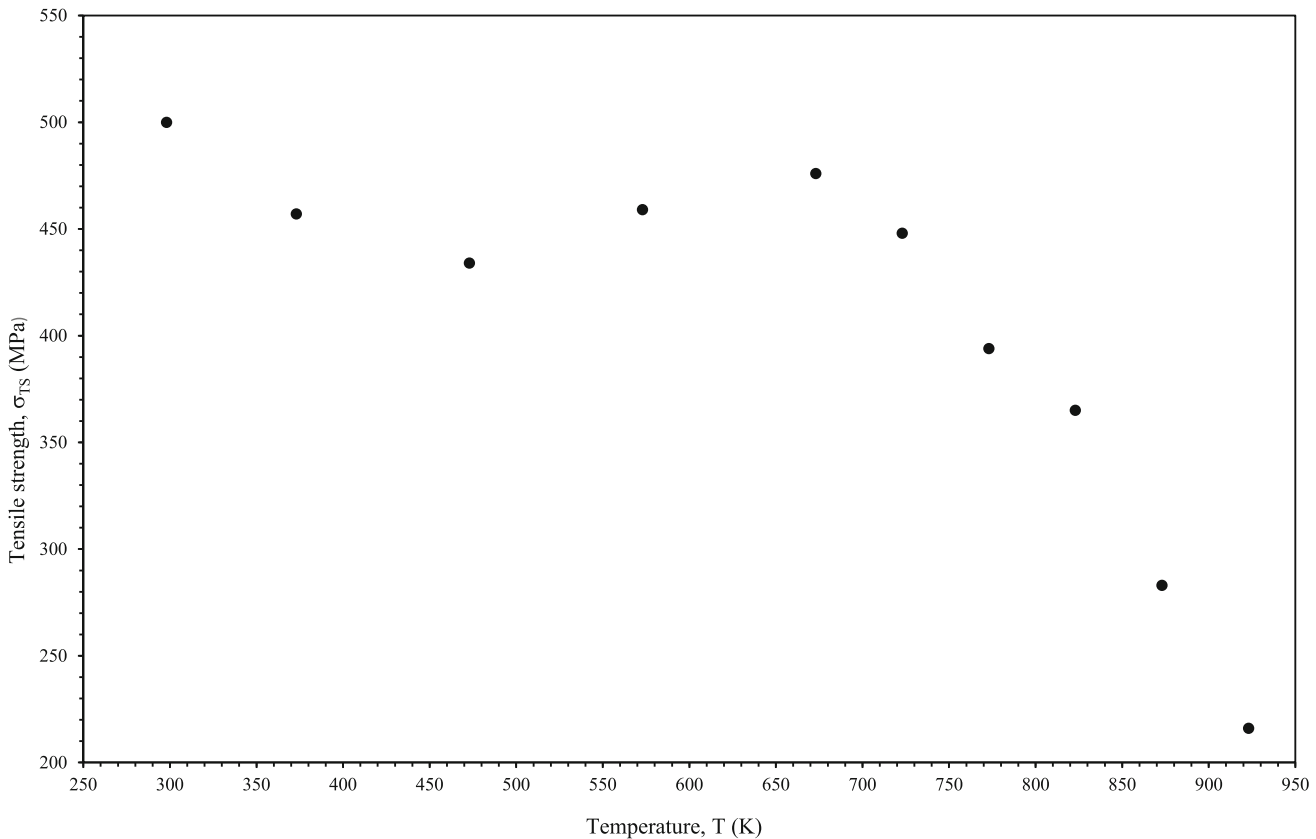


Fig. 2—Tensile strength values for the MAF batch of steel published by NIMS (strain rate =  $0.00125 \text{ s}^{-1}$ ).

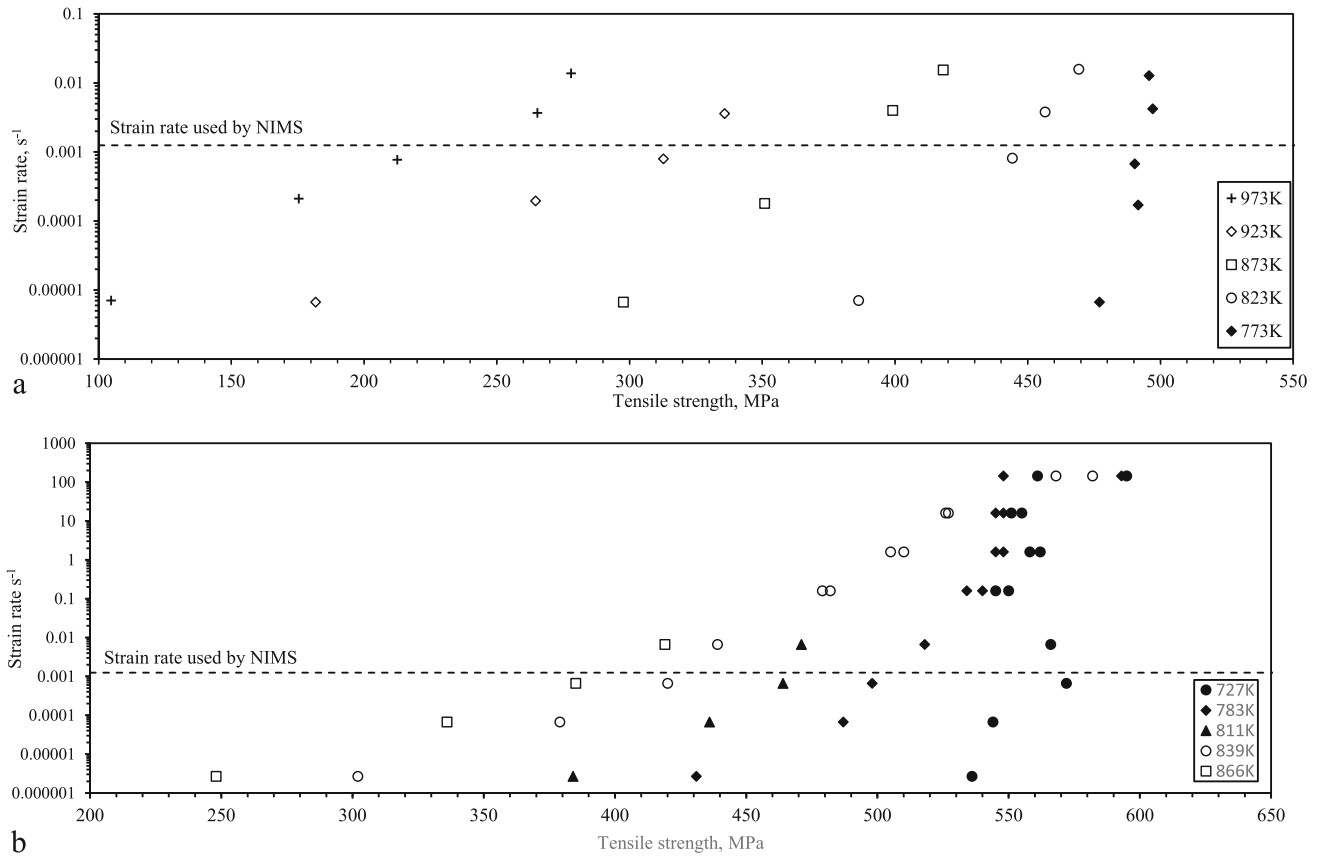


Fig. 3—Tensile strength values for the batch of steel studied by (a) Bueno and Sobrinho<sup>[9]</sup> and (b) Klueh and Oakes.<sup>[10]</sup>

are the approximate  $\sigma/\sigma_{TS}$  values associated with these data points. At normalized stresses exceeding 0.41, the slopes of the two lines are approximately equal and correspond to an estimated average activation energy of  $\widehat{Q}_c = 340 \text{ kJ mol}^{-1}$ . At normalized stresses below 0.24, the slopes of the three lines show a little more variability with an activation energy ranging between 144 and  $243 \text{ kJ mol}^{-1}$  with an average value of  $\widehat{Q}_c = 190 \text{ kJ mol}^{-1}$ .

While there is no way of testing whether these two activation energies are statistically significantly different from each other, the size of the difference between them suggests this is likely to be the case. And this would be consistent with creep mechanisms described for this material by Whittaker and Wilshire<sup>[12]</sup> and Whittaker and Harrison<sup>[13]</sup> (With just two data points to define each line in Figure 4, the uncertainty associated with each shown  $Q_c$  value is unquantifiable. Nor is it possible to attach confidence bounds to their averages because it depends in part on the standard error of each  $Q_c$  value in Figure 4).

Whittaker and Wilshire<sup>[12]</sup> argued that at the highest stresses (corresponding to stresses above the materials yield stress) new dislocations multiply rapidly during the initial strain on loading, *i.e.*, plastic deformation takes place by a dislocation glide mechanism. Thereafter, dislocation creep begins where the main obstacle to their movement is the changed dislocation substructure upon

high stress loading. Over medium stresses (where the stress is below the yield stress), specimens deform elastically upon loading and the dislocation substructure remains mainly as it was before testing begins. Dislocation creep must occur not so much by the generation of new dislocations but more by the movement of the dislocations pre-existing in the as-received bainitic microstructure. Dislocation creep is therefore present from the start with the main obstacles to their movement being precipitates such as  $M_2C$ -type carbides. The lowest stress regime is characterized by very long test durations that degrade the initial bainitic microstructure—the original lath-like structure entirely disappears. This could explain the lower activation energy seen in Figure 4 at the lowest stresses.

### B. The Maximum Stresses, $\alpha$ and $\beta$

Using the above estimates for  $Q_c$ , Eq. [1a] can be written as (including an error term  $\varepsilon$  to pick up the experimental scatter)

$$\ln[\dot{\varepsilon}_M] + \widehat{Q}_c \left[ \frac{1}{RT} \right] = \ln[A] - n \ln[\tau] + \varepsilon. \quad [2]$$

Then values for  $A$ ,  $n$ , and  $\sigma_{\max}$  can be estimated as follows. First, choose starting values for  $\sigma_{\max}$  to quantify  $\tau$ , and then use the technique of linear least squares (LLS) to determine values for parameters  $A$  and

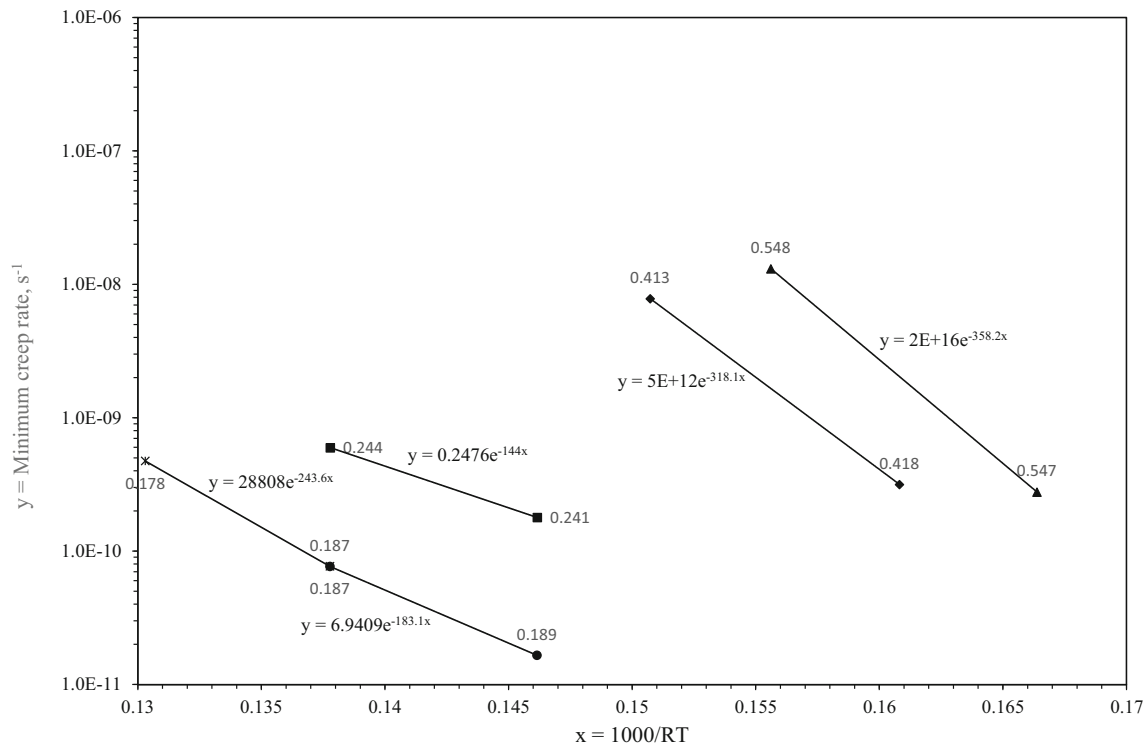


Fig. 4—Plot of  $\ln \dot{\epsilon}_M$  against  $1000/RT$  (gradients of shown lines correspond to creep activation energy).

$n$ . Thus, these two parameters are given values that minimize the sum of the squared  $\epsilon$  values, *i.e.*, minimize the residual sum of squares (RSS). New values for  $\sigma_{\max}$  can then be selected to redefine  $\tau$  in Eq. [2] and LLS used again to re-minimize the RSS. If the new RSS is lower than the original one, the selected  $\sigma_{\max}$  values are taken to be better than the original ones. This search over many different values for  $\sigma_{\max}$  can be structured using a non-linear search algorithm such as Excels Solver.<sup>[14]</sup> The estimates for  $\sigma_{\max}$  are those values that result in the smallest RSS over this search grid. The discontinuities in the data (caused by  $Q_c$  changing with stress and the possibility of  $A$  and  $n$  changing with stress) can be dealt with by applying Eq. [2] separately to the different stress ranges where the data on  $\ln[\dot{\epsilon}_M] + \widehat{Q}_c \left[ \frac{1}{RT} \right] v \ln[\tau]$  give straight lines.

### C. Consequences of a Varying Activation Energy for Creep

There is a consequence to the activation energy being different at the very lowest stresses. It will make it challenging to use Eq. [1a] to predict small minimum creep rates using only the larger minimum creep rates—*i.e.*, make predictions from accelerated tests. If the smaller rates are not known, it is impossible to estimate the lower activation energy at the lower stresses. However, as the start of tertiary creep comes before the time to failure, one approach would be to modify the nature of the accelerated test program. Instead of accelerating the stresses and temperatures to

induce quick failure, the test program could use much lower stresses and or temperatures and end the test when the minimum creep rate can be identified. This will still be a shorter-term test program as tertiary creep starts well before failure. Such an exercise could form part of future work, but it prevents extrapolation exercises being carried out in this paper. Thus, the following analysis uses all the NIMS data to evaluate how well Eq. [1a] characterizes the whole data set.

## V. RESULTS WHEN USING ALL THE NIMS DATA

The results of estimating Eq. [1a] using all the NIMS data and substituting in the NIMS values of  $\sigma_{TS}$  for  $\sigma_{\max}$  in Eq. [1a] are shown in Figure 5. It was found that the  $R^2$  value is maximized when  $k = 1$ , suggesting the Logistic S curve model represents the creep data better than the Weibull S curve model (hence the vertical axis shows  $\ln[(\sigma_{\max}/\sigma) - 1]$ ). The models fit or interpolated predictions are shown by the solid segmented line with 2 breaks points and this fit to the data is excellent—with an  $R^2$  value of 99.91 pct. The break at  $\ln(\tau) = 1.3$  corresponds to the change in activation energy. The resulting slopes of the lines in the highest and low stress regimes are then very similar ( $n$  in the range  $-2$  to  $-3$ ). The slope of the line in the intermediate stress range is  $n = -11.4$ .

The results of estimating Eq. [1a] using all the NIMS data and when estimating  $\sigma_{\max}$  using the approach described above are shown in Figure 6. It was again

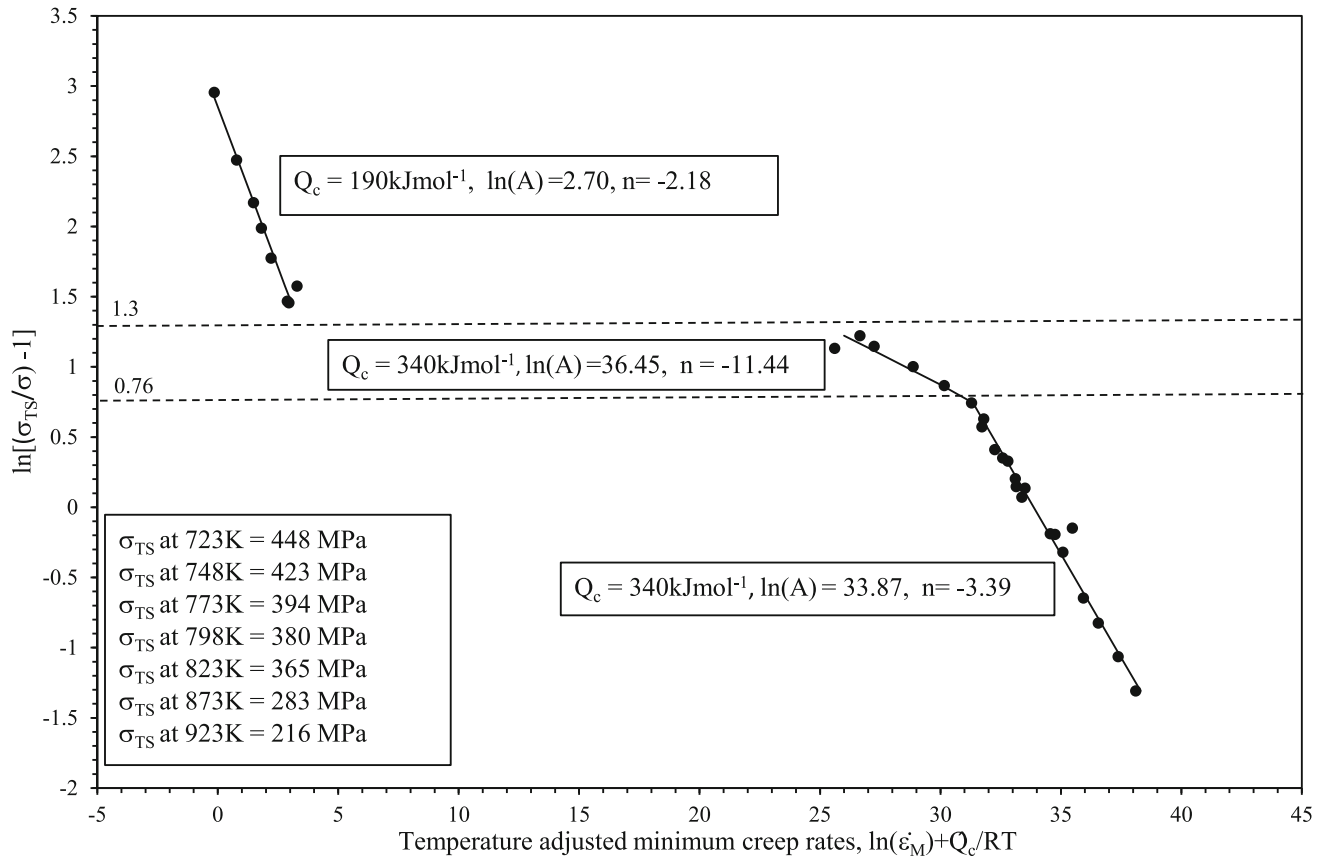


Fig. 5—The Logistic S curve representation of minimum creep rates using  $\sigma_{TS}$  from NIMS for  $\sigma_{max}$  in Eq. [1a].

found that the  $R^2$  value is maximized when  $k = 1$ , suggesting the Logistic S curve model represents the creep data better than the Weibull S curve model. The models fit or interpolated predictions are shown by the solid segmented line with 2 breaks points and this fit to the data is excellent—with an  $R^2$  value of 99.91 pct. The break at  $\ln(\tau) = 1.5$  again corresponds to the change in activation energy. The resulting slopes of the lines in the highest and low stress regimes are then very similar ( $n$  in the range  $-2$  to  $-4$ ). The slope of the line in the intermediate stress range is  $n = -11.3$ . It is interesting to note the values for the parameters  $A$  and  $n$  are little changed by estimating  $\sigma_{max}$ . A comparison of Figures 5 and 6 shows that the estimated values for  $\sigma_{max}$  are markedly higher at all temperatures—especially at lower temperatures and this is consistent with the results of, for example, Klueh and Oakes.<sup>[10]</sup>

These different characterizations of the NIMS minimum creep rates are further revealed in Figures 7 and 8. Figure 7 plots the two models' interpolations in the more familiar stress-time space. While the differences are not large, the S curve model that uses the estimated  $\sigma_{max}$  values clearly represent the entirety of the data best and this is most clearly seen at higher temperatures. This is further revealed in Figure 8 which plots the interpolations from the two models against the actual minimum creep rates.

Again, the differences are visually small, but these are different representations. For the model that uses the NIMS tensile strength values the trend line differs from an ideal 45 deg line. The power term of the trend line is close to 1 (1.01) and so this trend line equation reveals that on average the actual minimum creep rates are some 2.24 times larger than the model's interpolations. For the model that is based on estimated values for  $\sigma_{max}$ , the trend line again differs from an ideal 45 deg line, but by a smaller amount. The power term is again close to 1 (1.003) and so this trend line equation reveals that on average the actual minimum creep rates are some 1.07 times larger than the model's interpolations. What is more, the  $R^2$  value of this trend line is substantially higher indicating that this model has much less scatter around the interpolated lines—there is less random variation around the interpolation curves shown in Figure 7. Thus, the S-shaped curve model represents the data better when the NIMS tensile strength values are abandoned.

## VI. CONCLUSIONS

This paper has highlighted the possibility that the  $\sigma_{TS}$  values published by NIMS on 2.25Cr-1Mo steel

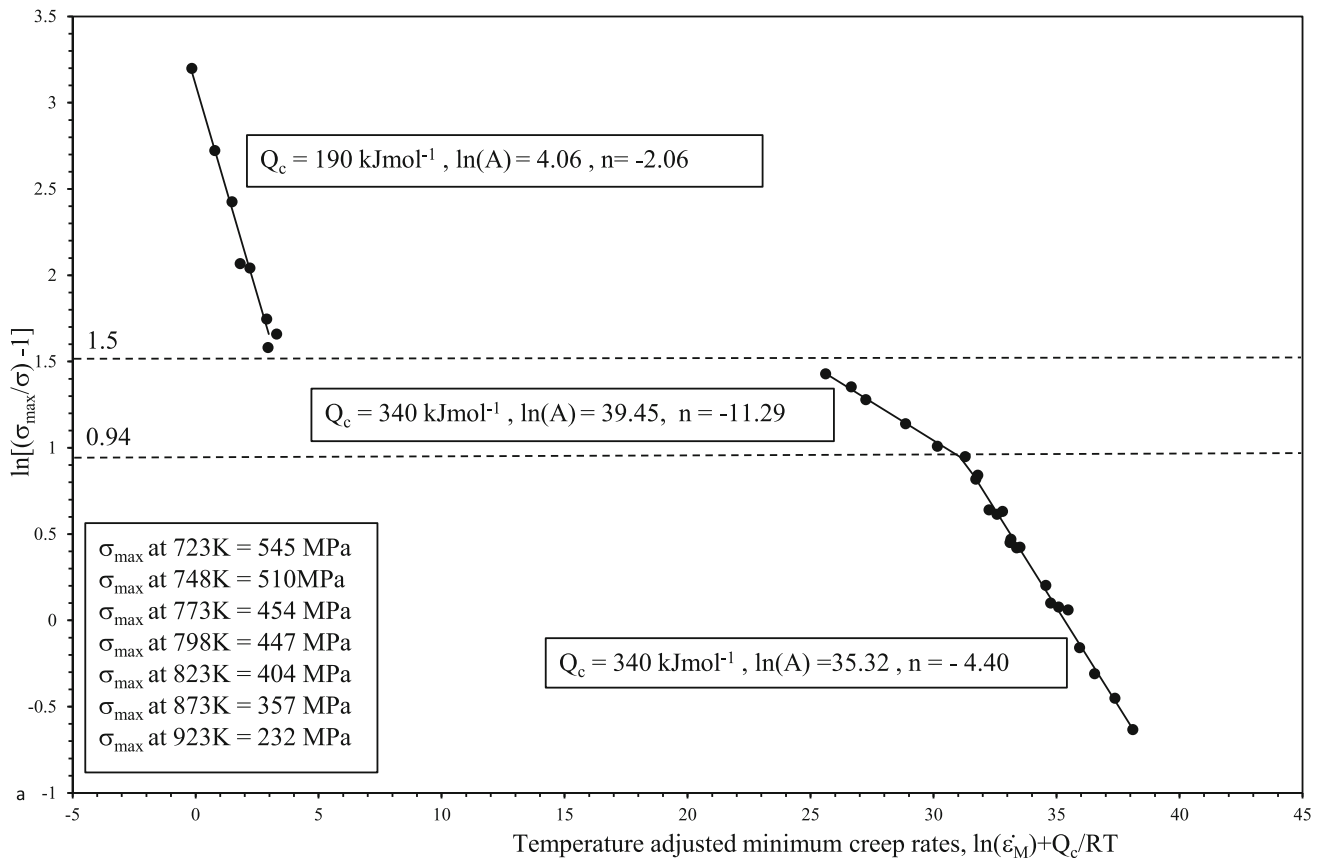


Fig. 6—The Logistic S curve representation of minimum creep rates using estimates of  $\sigma_{\max}$  instead of  $\sigma_{TS}$  from NIMS in Eq. [1a].

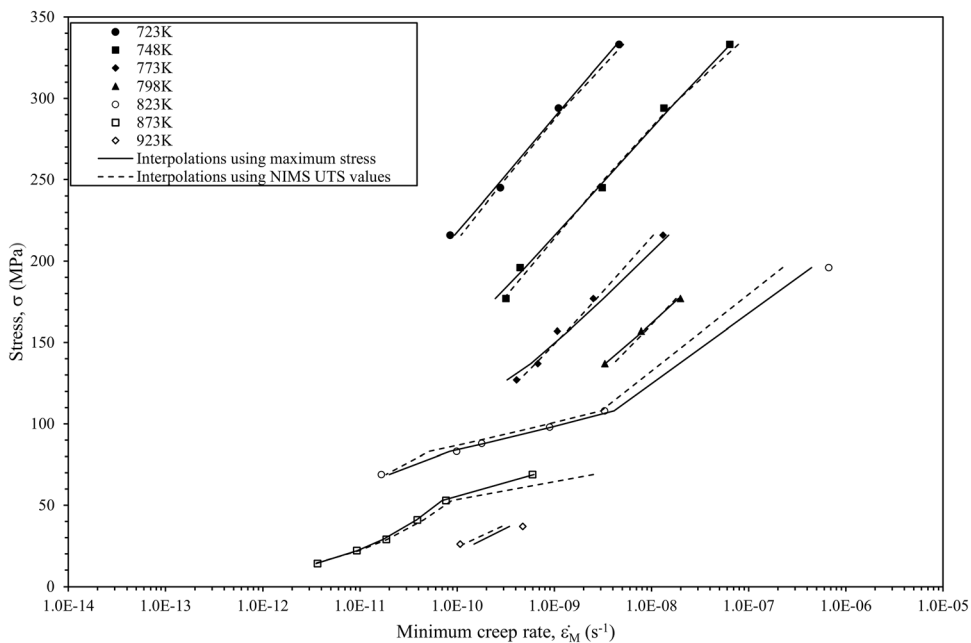


Fig. 7—The Logistic S curve models interpolations of  $\dot{\epsilon}_M$  at various stresses and temperatures together with the actual  $\dot{\epsilon}_M$  values.

may not be suitable values for  $\sigma_{\max}$  in S-shaped curve models of creep because the strain rate used by NIMS in their high-temperature tensile testing is too low.

The paper proposed the replacement of NIMS  $\sigma_{TS}$  values with a maximum stress estimated directly from the creep data itself. This modified model was then applied to data obtained by NIMS on 2.25Cr-1Mo

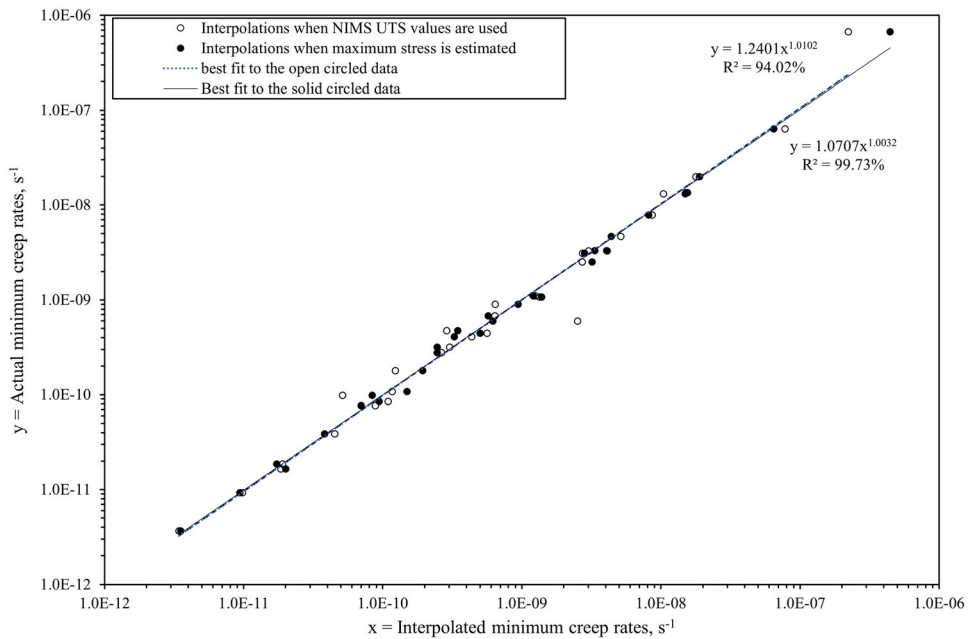


Fig. 8—Plot of the Logistic S curve models interpolations of  $\dot{\epsilon}_M$  against the actual  $\dot{\epsilon}_M$  values.

steel. The main findings from this approach are as follows:

1. The  $\sigma_{TS}$  values for this material were shown to be strain rate dependent even at very high strain rates and certainly at the strain rates used by NIMS in their high-temperature tensile testing. This is consistent with this paper's findings that the estimated values for  $\sigma_{max}$  obtained using the Logistic S curve model are much higher than those published by NIMS.
2. When these  $\sigma_{TS}$  values are replaced by  $\sigma_{max}$  using the estimation procedure developed in this paper, there is an improved representation of the minimum creep rate data. The interpolations are closer to the actual values and there is less random scatter.
3. The Logistic S curve creep model represents the NIMS creep data better than the Weibull S curve model.
4. Two activation energies were identified, with the lower value being associated with microstructure degradation, the result of prolonged testing at low stresses.

This last point has implications for the nature of accelerated testing when the aim of such testing is to life materials. Instead of accelerating the stresses and temperatures to induce quick failure, test programs on 2.25Cr-1Mo steel should use much lower stresses and or temperatures than these accelerated values, and the tests should run only until the minimum creep rate is identified. These will still be a shorter-term test program as tertiary creep starts well before failure. Such an exercise could form part of future work. It would also be useful to apply this procedure for estimating  $\sigma_{max}$  to

materials (such as 1Cr steel) where there is not a fall in the activation energy at long test durations to see if the use of  $\sigma_{max}$  improves extrapolative performance as well as the interpolative performance observed in this paper. Also, more experimental work is encouraged into verifying the most appropriate strain rates to be used in tensile testing when the purpose is to use the resulting  $\sigma_{TS}$  values for use in S-shaped curve models. This will require more high-temperature tensile testing at relatively high constant strain rates to determine the strain rate at which  $\sigma_{TS}$  becomes invariant to further increases in the strain rate.

#### DATA AVAILABILITY

All data used in this publication are in the public domain: References 8 through 11.

#### CONFLICT OF INTEREST

This research was not funded by research council grant or private sponsors and as such there are no financial relationships to declare.

#### OPEN ACCESS

This article is licensed under a Creative Commons Attribution 4.0 International License, which permits use, sharing, adaptation, distribution and reproduction in any medium or format, as long as you give appropriate credit to the original author(s) and the source, provide a link to the Creative Commons licence, and indicate if changes were made. The images or other third party material in this article are included in the

article's Creative Commons licence, unless indicated otherwise in a credit line to the material. If material is not included in the article's Creative Commons licence and your intended use is not permitted by statutory regulation or exceeds the permitted use, you will need to obtain permission directly from the copyright holder. To view a copy of this licence, visit <http://creativecommons.org/licenses/by/4.0/>.

## REFERENCES

1. Boiler and Pressure Vessel Code, ASME, New York, 2004. 450.
2. D. Allen and S. Garwood: *Energy Materials-Strategic Research Agenda*, 2007. [http://www.matuk.co.uk/docs/1\\_StrategicResearchAgenda%20FINAL.pdf](http://www.matuk.co.uk/docs/1_StrategicResearchAgenda%20FINAL.pdf). Accessed 28 May 2019.
3. F.C. Monkman and N.J. Grant: *Proc. Am. Soc. Test. Mater.*, 1956, vol. 56, p. 593.
4. M. Evans: *Metall. Mater. Trans. A*, 2020, vol. 51A, pp. 697–707.
5. M. Yang, Q. Wang, X.L. Song, J. Jia, and Z.D. Xiang: *Int. J. Mater. Res.*, 2016, vol. 107(2), pp. 133–38.
6. Q. Wang, M. Yang, X.L. Song, J. Jia, and Z.D. Xiang: *Metall. Mater. Trans. A*, 2016, vol. 48A(7), pp. 3479–87.
7. B. Wilshire and A.J. Battenbough: *Mater. Sci. Eng. A*, 2007, vol. 443, pp. 156–66.
8. NIMS Creep Data Sheet No. 3B: Data Sheets on the Elevated-Temperature Properties of 2.25Cr-1Mo Steel for Boiler and Heat Exchanger Seamless Tubes (STBA 24), National Research Institute for Metals, Tokyo, Japan.
9. J.F. dos Reis Sobrinho and L. de Oliveira Bueno: *Revista Matéria*, 2005, vol. 10(3), pp. 463–71.
10. R.L. Klueh and R.E. Oakes: *J. Eng. Mater. Technol.*, 1977, vol. 88, pp. 350–57.
11. NIMS Creep Data Sheet No.50A: Long-Term Creep Rupture Data obtained after Publishing the Final Edition of the Creep Data Sheets, National Research Institute for Metals, Tokyo, Japan.
12. M. Whittaker and B. Wilshire: *Mater. Sci. Eng. A*, 2010, vol. 527(18–19), pp. 4932–38.
13. M. Whittaker and W.J. Harrison: *Mater. High Temp.*, 2014, vol. 31(3), pp. 233–38.
14. Microsoft Corporation. Microsoft Excel. 2018. <https://office.microsoft.com/excel>.

**Publisher's Note** Springer Nature remains neutral with regard to jurisdictional claims in published maps and institutional affiliations.